

Nonlinear Energy Response of Glass Forming Materials

Fumitaka Tagawa* and Takashi Odagaki

Department of Physics, Kyushu University, Fukuoka 812-8581, Japan.

(Dated: March 29, 2017)

Abstract

A theory for the nonlinear energy response of a system subjected to a heat bath is developed when the temperature of the heat bath is modulated sinusoidally. The theory is applied to a model glass forming system, where the landscape is assumed to have 20 basins and transition rates between basins obey a power law distribution. It is shown that the statistics of eigenvalues of the transition rate matrix, the glass transition temperature T_g , the Vogel-Fulcher temperature T_0 and the crossover temperature T_x can be determined from the 1st- and 2nd-order ac specific heats, which are defined as coefficients of the 1st- and 2nd-order energy responses. The imaginary part of the 1st-order ac specific heat has a broad peak corresponding to the distribution of the eigenvalues. When the temperature is decreased below T_g , the frequency of the peak decreases and the width increases. Furthermore, the statistics of eigenvalues can be obtained from the frequency dependence of the 1st-order ac specific heat. The 2nd-order ac specific heat shows extrema as a function of the frequency. The extrema diverge at the Vogel-Fulcher temperature T_0 . The temperature dependence of the extrema changes significantly near T_g and some extrema vanish near T_x .

I. INTRODUCTION

Since the anomaly of the specific heat at the glass transition was discovered in 1923¹, many studies have been conducted to understand the behavior. Since the anomaly depends on the measurement process, the transition is now believed not to be understood in the framework of the standard thermodynamics².

Recently the concept of the landscape has been paid much attention because of possibility to explain the transition in non-equilibrium systems^{3,4}. In particular, the free energy landscape (FEL) picture proposed by Odagaki et al^{5,6} is considered to provide the unified concept for understanding thermodynamic and dynamic singularities of the glass transition. In fact, the single particle dynamics⁷ and the specific heat^{8,9,10,11,12,13,14} were shown to phenomenologically be well described by the framework based on the FEL. Namely, the dynamical transition is understood as the Gaussian-to-Non-Gaussian transition⁷, and the thermodynamic singularities near T_g , including the cooling rate dependence of the specific heat, is characterized as the Quenched-to-Annealed transition in dynamics on the FEL^{8,9,10,11}.

The specific heat of non-equilibrium systems such as glass forming materials is defined by the reponse of the energy to the unit rise of temperature¹⁵. Because of the slow relaxations, the system cannot reach equilibrium during the measurement and the energy response shows the time delay. Therefore one can expect that the ac specific heat^{16,17} will contain informations of the slow dynamics. The ac specific heat $\tilde{C}_1(i\omega)$ is defined as the Laplace-Fourier transform of the energy or enthalpy correlation function $\phi(t)$ ^{14,18}

$$\tilde{C}_1(i\omega) = \int_0^\infty dt \phi(t) e^{-i\omega t}. \quad (1)$$

The ac specific heat is often fitted by the Laplace-Fourier transform of the stretched exponential $\phi(t) = \exp\left(- (t/\tau)^\beta\right)$, since the correlation function is believed to be the superposition of the Debye relaxation function with different relaxation times. However the origin of the distribution of the relaxation times has not clearly been understood.

So far, studies of the energy response of glass forming systems have been limited within the linear response region, and the nonlinear energy response has not been studied yet. In a previous paper¹⁴, we proposed the description of the 1st- and 2nd-order energy response with the free energy landscape picture and applied it to a two level system with a diverging barrier. It is shown that the 2nd-order energy response has a diverging term at the temperature where the relaxation time diverges.

In this paper, we investigate the linear and nonlinear energy responses of non-equilibrium systems described by the FEL picture to an oscillating temperature and present the characteristic behavior of the 1st- and 2nd-order ac specific heat. Using a model FEL which supports a glass transition, we show that the Vogel-Fulcher temperature and the cross-over temperature as well as the glass transition temperature can be determined from the characteristic behavior of the ac specific heats. We also show that the statistics of the transition rate matrix representing the stochastic dynamics among the basins of the FEL can be obtained from the frequency dependence of the 1st-order ac specific heat.

The organization of the paper is as follows: In §2, we explain the 1st- and 2nd-order energy responses when the temperature of the heat bath is oscillated sinusoidally. The definition of the 1st- and 2nd-order ac specific heat is also given. In §3, the stochastic dynamics on the free energy landscape is explained. In §4, we describe the 1st- and 2nd-order energy responses to the oscillating temperature and the 1st- and 2nd-order ac specific heats when the system is described by the FEL picture. As an example, a model system with FEL consisting of 20 basins is analyzed. In §5, where transition rates between basins are assumed to obey a power law distribution. We present the characteristics of the 1st- and 2nd-order ac specific heats of the glass former and show that the glass transition temperature, the Vogel-Fulcher temperature and the crossover temperature can be determined by the ac specific heats. In §6, our conclusion is given.

II. THE FIRST AND SECOND ORDER SPECIFIC HEATS

The specific heat at the constant volume C_V is conventionally defined by a derivative of the energy with respect to the temperature,

$$C_V(T) = \left(\frac{\partial E_{\text{eq}}}{\partial T} \right)_V, \quad (2)$$

where E_{eq} is the energy in the equilibrium state, T is the temperature and V is the volume. In this discussion of the specific heat, it is not considered how long the system takes to equilibrate itself when the temperature is changed. When the system contains degrees of freedom of slow dynamics, one must consider the effect of the delay in response. We consider the energy response of a system with slow relaxations which is subjected to a heat bath whose temperature is oscillated as $T + \Delta T(t)$, where T is the average temperature and $\Delta T(t)$ is

the oscillating part. We assume that the energy response $\Delta E(t)$ can be expanded as follows:

$$\begin{aligned}\Delta E(t) &= \int_{-\infty}^t dt_1 C_1(t-t_1) \Delta T(t_1) \\ &+ \int_{-\infty}^t dt_1 \int_{-\infty}^t dt_2 C_2(t-t_1, t-t_2) \Delta T(t_1) \Delta T(t_2) + O(\Delta T^3),\end{aligned}\quad (3)$$

where C_1 and C_2 represent the retardation effect of the system.

The Fourier transform $\Delta E(\omega)$ of Eq. (3) is given by

$$\begin{aligned}\Delta E(\omega) &= \tilde{C}_1(i\omega) \Delta T(\omega) \\ &+ \int_{-\infty}^{\infty} d\omega_1 \tilde{C}_2(i\omega_1, i\omega - i\omega_1) \Delta T(\omega_1) \Delta T(\omega - \omega_1) + O(\Delta T^3),\end{aligned}\quad (4)$$

where the Laplace components $\tilde{C}_1(p)$ and $\tilde{C}_2(p_1, p_2)$ are defined by

$$\tilde{C}_1(p) = \int_0^{\infty} dt C_1(t) e^{-pt}, \quad (5)$$

$$\tilde{C}_2(p_1, p_2) = \int_0^{\infty} dt_1 \int_0^{\infty} dt_2 C_2(t_1, t_2) e^{-p_1 t_1} e^{-p_2 t_2}, \quad (6)$$

and $\Delta T(\omega)$ is the Fourier transform of $\Delta T(t)$.

We now discuss the energy response $\Delta E(t)$ when $\Delta T(t)$ is a sinusoidal function $\Delta T(t) = T_a \sin(\omega t)$, where T_a is the amplitude of the oscillating temperature. It is straightforward to show that

$$\begin{aligned}\Delta E(t) &= T_a \{ \tilde{C}'_1(i\omega) \sin(\omega t) + \tilde{C}''_1(i\omega) \cos(\omega t) \} \\ &- \frac{T_a^2}{2} \{ \tilde{C}'_2(i\omega, i\omega) \cos(2\omega t) - \tilde{C}''_2(i\omega, i\omega) \sin(2\omega t) - \tilde{C}'_2(i\omega, -i\omega) \} + O(T_a^3).\end{aligned}\quad (7)$$

Here $C_1(t)$ and $C_2(t_1, t_2)$ are assumed to be real and the notations ' and '' represent the real and imaginary parts, respectively. The coefficients of the 1st-order temperature term, $\tilde{C}'_1(i\omega)$ and $\tilde{C}''_1(i\omega)$ are known as the real and imaginary parts of the (1st-order) ac specific heat, which was introduced by Birge and Nagel¹⁶ and by Christensen¹⁷.

The 2nd-order temperature term consists of the oscillating and nonoscillating terms. We define the 2nd-order ac specific heat $\tilde{C}'_2(i\omega, i\omega)$ and $\tilde{C}''_2(i\omega, i\omega)$ by the coefficients of the oscillating term.

The Laplace-Fourier transforms $\tilde{C}_1(p)$ and $\tilde{C}_2(p_1, p_2)$ are related to the temperature derivative of the energy. When the change of the temperature is slower than that of the

time scale of the retardation effects $C_1(t)$ and $C_2(t_1, t_2)$, it is straightforward to obtain the following expressions,

$$\lim_{p \rightarrow 0} \tilde{C}_1(p) = \int_0^\infty dt C_1(t) = \frac{\partial E_{eq}}{\partial T} \quad (8)$$

$$\lim_{p_1 \rightarrow 0} \lim_{p_2 \rightarrow 0} \tilde{C}_2(p_1, p_2) = \int_0^\infty dt_1 \int_0^\infty dt_2 C_2(t_1, t_2) = \frac{1}{2} \frac{\partial^2 E_{eq}}{\partial T^2}. \quad (9)$$

When the frequency is smaller than the inverse of the structural relaxation time, the energy responses without delay and $\Delta E(t)$ can be expressed as

$$\Delta E(t) = \frac{\partial E_{eq}}{\partial T} \Delta T(t) + \frac{1}{2} \frac{\partial^2 E_{eq}}{\partial T^2} \Delta T^2(t) + O(\Delta T^3). \quad (10)$$

In this limit, $\tilde{C}'_1(i\omega)$ becomes equal to the specific heat in the equilibrium state, $C_V = \partial E_{eq}/\partial T$ and $\tilde{C}''_1(i\omega)$ vanishes. It can also be confirmed that in this limit $\tilde{C}_2(i\omega, i\omega)$ and $\tilde{C}_2(i\omega, -i\omega)$ corresponds to the temperature derivative of the specific heat. These behaviors are consistent with Eqs. (8) and (9).

III. DYNAMICS ON THE FREE ENERGY LANDSCAPE

The free energy surface in the configurational space is defined by the partial partition function which is given by the partial summation of the phase space spanned by the fast microscopic motion^{5,6}, and the slow dynamics is represented by the stochastic motion on the free energy surface. Around the glass transition point, the stochastic motions can be classified into two types; the fluctuation in one basin due to the structural fluctuation around a certain structure and the transition between basins which corresponds to the structural relaxation.

Here, we concentrate on the transition between basins and ignore the fluctuation within a single basin. We denote the probability that the system is in basin i at time t at temperature T by $P_i(T, t)$ and a physical quantity A of basin i by $A_i(T)$. Then the physical quantity we measure at time t is defined as an average over the basins,

$$A(T, t) = \sum_i A_i(T) P_i(T, t) = \vec{A}(T) \cdot \vec{P}(T, t), \quad (11)$$

where $\vec{A}(T)$ and $\vec{P}(T, t)$ are the vectors consisting of components $A_i(T)$ and $P_i(T, t)$, respectively.

The probability vector $\vec{P}(T, t)$ is assumed to obey the master equation,

$$\frac{d}{dt}\vec{P}(T, t) = W(T)\vec{P}(T, t), \quad (12)$$

where $W(T)$ is the transition rate matrix, i.e. W_{ij} is the transition rate from basin j to i and $W_{ii} = -\sum_{j \neq i} W_{ji}$ is the transition rate jumping out from basin i . The transition rate is assumed to be related to the free energy barrier as follows,

$$W_{ij} = C \exp[-\beta(F_A(T) - F_j(T))], \quad (13)$$

where C is the attempt frequency of the jump motion, $\beta = 1/k_B T$ is the inverse of the temperature T multiplied by Boltzmann constant k_B , $F_i(T)$ is the free energy of basin i , $F_A(T) = \max\{F_i(T), F_j(T)\} + \Delta_{i,j}(T)$ and $\Delta_{i,j}(T)$ is the energy barrier between basin i and j . In the high temperature region, the transition rate is large and the system moves among basins freely. On the other hand, the transition rate becomes small and the structural transition is hindered at low temperatures.

The transition rate matrix W in the master equation (12) must satisfy the condition that the long time limit of $P_i(T, t)$ becomes the Boltzmann distribution

$$\lim_{t \rightarrow \infty} P_i(T, t) = P_i^{eq}(T) = \frac{\exp[-\beta F_i(T)]}{\sum_j \exp[-\beta F_j(T)]}. \quad (14)$$

Therefore, the transition rate matrix W obeys the following detailed balance

$$W\vec{P}^{eq} = 0. \quad (15)$$

When the temperature T does not depend on time, Eq. (12) can be readily solved

$$\begin{aligned} \vec{P}(T, t) &= \exp[W(T)t]\vec{P}(T, t=0) \\ &= V \begin{pmatrix} \exp(\lambda_1 t) & & & \\ & \ddots & & \\ & & \exp(\lambda_{N-1} t) & \\ & & & \exp(\lambda_N t) \end{pmatrix} V^{-1}\vec{P}(T, t=0), \end{aligned} \quad (16)$$

where N is the number of basins, λ_i is the i -th eigenvalue of W and V is a matrix whose columns are eigenvectors of W . It is important to note that there is an eigenvalue $\lambda_i = 0$ which corresponds to the detailed balance of Eq. (15).

IV. THE ENERGY RESPONSE TO THE OSCILLATING TEMPERATURE

A. The 1st- and 2nd-order energy response

The time dependent temperature $\hat{T}(t)$ is assumed to be $\hat{T}(t) = T + \Delta T(t)$, where T is the average temperature and $\Delta T(t)$ is the oscillating part of the temperature. The probability vector $\vec{P}(T, t)$ is expanded as

$$\vec{P}(\hat{T}(t), t) = \vec{P}_0(t) + \Delta\vec{P}_1(t) + \Delta\vec{P}_2(t) + O(\Delta T^3), \quad (17)$$

where $\Delta\vec{P}_n$ is the term of order ΔT^n . Note the explicit temperature dependence of the quantities on the right hand side of Eq. (17). is omitted. It is clear that $\vec{P}_0(t) = \vec{P}^{eq}(T)$. Then the 1st- and 2nd-order energy responses, $\Delta E_1(t)$ and $\Delta E_2(t)$ at time t are represented as

$$\Delta E_1(t) = \vec{E} \cdot \Delta\vec{P}_1(t) + \frac{\partial \vec{E}}{\partial T} \cdot \vec{P}_{eq}(T) \Delta T(t) \quad (18)$$

$$\Delta E_2(t) = \vec{E} \cdot \Delta\vec{P}_2(t) + \frac{\partial \vec{E}}{\partial T} \Delta\vec{P}_1(t) \Delta T(t) + \frac{1}{2} \frac{\partial^2 \vec{E}}{\partial T^2} \vec{P}_{eq}(T) \Delta T^2(t) \quad (19)$$

where \vec{E} is the vector consisting of components E_i . The 1st- and 2nd-order probability responses, $\Delta P_1(t)$ and $\Delta P_2(t)$, obey the following equations derived from Eq. (12),

$$\frac{d}{dt} \Delta\vec{P}_1(t) = W(T) \Delta\vec{P}_1(t) + \frac{\partial W(T)}{\partial T} \vec{P}_{eq}(T) \Delta T(t) \quad (20)$$

$$\frac{d}{dt} \Delta\vec{P}_2(t) = W(T) \Delta\vec{P}_2(t) + \frac{\partial W(T)}{\partial T} \Delta\vec{P}_1(t) \Delta T(t) + \frac{1}{2} \frac{\partial^2 W(T)}{\partial T^2} \vec{P}_{eq}(T) \Delta T(t)^2. \quad (21)$$

It is straightforward to solve Eqs. (20) and (21) as

$$\Delta\vec{P}_1(t) = \int_{-\infty}^t ds e^{W(t-s)} \frac{\partial W}{\partial T} \vec{P}_{eq}(T) \Delta T(s), \quad (22)$$

$$\begin{aligned} \Delta\vec{P}_2(t) = & \int_{-\infty}^t ds_1 \int_{-\infty}^{s_1} ds_2 e^{W(t-s_1)} \frac{\partial W}{\partial T} e^{W(s_1-s_2)} \frac{\partial W}{\partial T} \vec{P}_{eq}(T) \Delta T(s_1) \Delta T(s_2) \\ & + \frac{1}{2} \int_{-\infty}^t ds e^{W(t-s)} \frac{\partial^2 W}{\partial T^2} \Delta T^2(s). \end{aligned} \quad (23)$$

B. The 1st-order energy response and the ac specific heat

The (1st-order) ac specific heat is defined as the linear coefficient of the energy response to the temperature change¹². Comparing Eqs. (3), (18) and (22), the retardation effect of

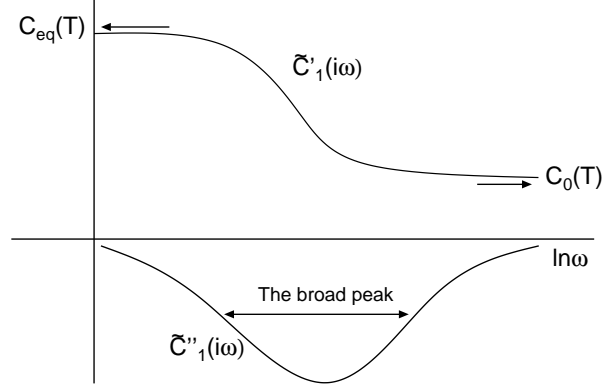


FIG. 1: The schematic picture of the (1st-order) ac specific heat in the free energy landscape picture.

the 1st-order energy response $C_1(t)$ is represented in the free energy landscape picture as follows,

$$C_1(t) = 2C_0(T)\delta(t) + \vec{E} \cdot \exp(Wt) \frac{\partial W}{\partial T} \vec{P}_{eq}, \quad (24)$$

where $C_0(T) = \vec{P}_{eq} \cdot \partial \vec{E} / \partial T$ is the quenched specific heat contributed only from the fast degree of freedom at one basin^{8,9,10,11,14}. The 2nd term represents the response from the transition between basins.

From Eq.(5), the 1st-order ac specific heat $\tilde{C}_1(i\omega)$ is given by the Laplace-Fourier transform of $C_1(t)$. The real part $\tilde{C}'_1(i\omega)$ and the imaginary part $\tilde{C}''_1(i\omega)$ are written as

$$\tilde{C}'_1(i\omega) = C_0(T) + \vec{E} \cdot V \begin{pmatrix} \lambda_1^2 / (\omega^2 + \lambda_1^2) & & \\ & \ddots & \\ & & \lambda_N^2 / (\omega^2 + \lambda_N^2) \end{pmatrix} V^{-1} \frac{\partial \vec{P}_{eq}}{\partial T}, \quad (25)$$

$$\tilde{C}''_1(i\omega) = \vec{E} \cdot V \begin{pmatrix} \lambda_1 \omega / (\omega^2 + \lambda_1^2) & & \\ & \ddots & \\ & & \lambda_N \omega / (\omega^2 + \lambda_N^2) \end{pmatrix} V^{-1} \frac{\partial \vec{P}_{eq}}{\partial T}. \quad (26)$$

The frequency dependence of the ac specific heat is shown in Fig.1 schematically. In the low frequency region, $\tilde{C}'_1(i\omega)$ approaches the specific heat in the equilibrium state as $C_{eq}(T) = \partial \vec{E} / \partial T \cdot \vec{P}_{eq} + \vec{E} \cdot \partial \vec{P}_{eq} / \partial T$ and $\tilde{C}''_1(i\omega)$ vanishes. This indicates the fact that the energy responds without time delay when the temperature is oscillated slowly. Since the eigenvalue λ_i is distributed, $\tilde{C}''_1(i\omega)$ has a broader peak than that of the Debye relaxation type

and $\tilde{C}'_1(i\omega)$ is represented as the sum of Lorentzian functions. This behavior is consistent with the measurement of the ac specific heat in glass forming materials¹⁶. In the high frequency region, $\tilde{C}'_1(i\omega)$ approaches $C_0(T)$ and $\tilde{C}''_1(i\omega)$ vanishes. It exhibits that the energy response within the 1st-order temperature perturbation is determined by the energy change in a basin alone when the temperature fluctuates rapidly.

The 1st-order ac specific heat can be used as the method to obtain the statistics of eigenvalues λ_i . From Eqs.(25) and (26), the scaled 1st-order ac specific heat is related to the distribution of the eigenvalues λ_i of the transition rate matrix as follows,

$$\frac{\tilde{C}'_1(i\omega) - C_0}{C_{eq} - C_0} = \sum_i g_i \frac{\lambda_i^2}{\lambda_i^2 + \omega^2}, \quad (27)$$

$$\frac{\tilde{C}''_1(i\omega)}{C_{eq} - C_0} = \sum_i g_i \frac{\lambda_i \omega}{\omega^2 + \lambda_i^2}. \quad (28)$$

Here, g_i is a factor related to the vectors \vec{E} , \vec{P}_{eq} and V given by

$$g_i = \frac{\sum_{j,k} E_i V_{ji} V_{ik}^{-1} \frac{\partial P_{eq}^k}{\partial T}}{C_{eq} - C_0}. \quad (29)$$

In the small frequency region, the imaginary part behaves as $\lim_{\omega \rightarrow 0} \tilde{C}''_1(i\omega)/(C_{eq} - C_0) = \sum_i g_i \lambda_i^{-1} \omega$. In the high frequency region, the real part behaves as $\lim_{\omega \rightarrow \infty} (\tilde{C}'_1(i\omega) - C_0)/(C_{eq} - C_0) = \sum_i g_i \lambda_i^2/\omega^2$ and the imaginary part behaves as $\lim_{\omega \rightarrow \infty} \tilde{C}''_1(i\omega)/(C_{eq} - C_0) = \sum_i g_i \lambda_i \omega^{-1}$. We can estimate $\sum_i g_i \lambda_i$, $\sum_i g_i \lambda_i^2$ and $\sum_i g_i \lambda_i^{-1}$ from the frequency dependence of the scaled 1st-order ac specific heat. These properties correspond to $\langle \lambda \rangle$, $\langle \lambda^2 \rangle$ and $\langle \lambda^{-1} \rangle$ respectively as will be shown in Sec. V.

C. The 2nd-order ac specific heat

The retardation effect of the 2nd-order energy response $C_2(t_1, t_2)$ is represented from Eqs. (3), (19) and (23) as

$$\begin{aligned} C_2(t_1, t_2) = & 2 \frac{\partial C_0}{\partial T} \delta(t_1) \delta(t_2) + \vec{E} \cdot \exp(Wt_1) \frac{\partial W}{\partial T} \exp(Wt_2) \frac{\partial W}{\partial T} \vec{P}^{eq} \theta(t_2 - t_1) \\ & + \frac{1}{2} \vec{E} \cdot \exp(Wt_1) \frac{\partial^2 W}{\partial T^2} \vec{P}^{eq} \delta(t_1 - t_2) + 2 \frac{\partial \vec{E}}{\partial T} \exp(Wt_1) \frac{\partial W}{\partial T} \vec{P}^{eq} \delta(t_2). \end{aligned} \quad (30)$$

The 1st term expresses the response due to the instant change of the specific heat of each basin and the remaining terms correspond to the effect of the transition motion between basins. Here, $\delta(x)$ is the Dirac's delta function and $\theta(x)$ is the Heaviside step function.

From the definition (6), the Laplace transform $\tilde{C}_2(p_1, p_2)$ is represented as

$$\begin{aligned} \tilde{C}_2(p_1, p_2) = & \frac{1}{2} \frac{\partial C_{eq}}{\partial T} - p_2 \vec{E} \cdot ((p_1 + p_2)\hat{1} - W)^{-1} \frac{\partial W}{\partial T} (p_2\hat{1} - W)^{-1} \frac{\partial \vec{P}^{eq}}{\partial T} \\ & - \frac{p_1 + p_2}{2} \vec{E} \cdot ((p_1 + p_2)\hat{1} - W)^{-1} \frac{\partial^2 \vec{P}^{eq}}{\partial T^2} - p_1 \frac{\partial \vec{E}}{\partial T} (p_1\hat{1} - W)^{-1} \frac{\partial \vec{P}^{eq}}{\partial T} \end{aligned} \quad (31)$$

The 2nd-order ac specific heats, which are introduced in eq. (3) by the coefficients of the oscillating term in the 2nd-order energy response, $\tilde{C}_2(i\omega, i\omega) = \tilde{C}'_2(i\omega, i\omega) + i\tilde{C}''_2(i\omega, i\omega)$ are expressed as

$$\begin{aligned} \tilde{C}'_2(i\omega, i\omega) = & \frac{1}{2} \frac{\partial C_{eq}}{\partial T} - 2\omega^2 \vec{E} \cdot (W^2 + 4\omega^2)^{-1} \frac{\partial^2 \vec{P}^{eq}}{\partial T^2} \\ & + \omega^2 \vec{E} \cdot (W^2 + 4\omega^2)^{-1} \left\{ 2 \frac{\partial W}{\partial T} W + W \frac{\partial W}{\partial T} \right\} (W^2 + \omega^2)^{-1} \frac{\partial \vec{P}^{eq}}{\partial T} \\ & - \omega^2 \frac{\partial \vec{E}}{\partial T} (W^2 + \omega^2)^{-1} \frac{\partial \vec{P}^{eq}}{\partial T}, \end{aligned} \quad (32)$$

$$\begin{aligned} \tilde{C}''_2(i\omega, i\omega) = & \omega \vec{E} \cdot W (W^2 + 4\omega^2)^{-1} \frac{\partial^2 \vec{P}^{eq}}{\partial T^2} \\ & + \omega \vec{E} \cdot (W^2 + 4\omega^2)^{-1} \left\{ 2\omega^2 \frac{\partial W}{\partial T} - W \frac{\partial W}{\partial T} W \right\} (W^2 + \omega^2)^{-1} \frac{\partial \vec{P}^{eq}}{\partial T} \\ & + \omega \frac{\partial \vec{E}}{\partial T} (W^2 + \omega^2)^{-1} \frac{\partial \vec{P}^{eq}}{\partial T}. \end{aligned} \quad (33)$$

In the low frequency limit, $\tilde{C}'_2(i\omega, i\omega)$ becomes $(\partial C_{eq}/\partial T)/2$ and $\tilde{C}''_2(i\omega, i\omega)$ vanishes. In the high frequency limit, $\tilde{C}'_2(i\omega, i\omega)$ is equal to $(\partial C_0/\partial T)/2$ and $\tilde{C}''_2(i\omega, i\omega)$ vanishes. These behaviors are qualitatively similar to those of the 1st-order ac specific heat. It indicates that the structural change of the system can catch up with the temperature change in the small frequency region and can not in the high frequency region.

Terms including the differential of the transition rate with respect to the temperature, $\partial W/\partial T$, is expected to show the characteristic behavior in the low temperature region, where the transition matrix W depends strongly on the temperature change. This characteristic does not appear in the 1st-order ac specific heat. In the high temperature region, the temperature dependence of the transition rate matrix W is weak. Therefore, the terms including $\partial W/\partial T$ are negligible, and the 2nd-order ac specific heat becomes the superposition of the susceptibility of the Debye relaxation. We explain this behavior for a trap model in the next section.

The 2nd-order energy response can be measured in the materials, where the derivatives of the quenched and equilibrium specific heats are much different, since the order of the 2nd-

order energy response is the difference between derivatives of these specific heats, $\partial(C_{eq} - C_0)/\partial T$.

V. APPLICATION TO A MODEL FREE ENERGY LANDSCAPE OF GLASS FORMING SYSTEMS

A. Model

To clarify the characteristics of the 1st- and 2nd-order ac specific heat of glass forming materials, we apply the present analysis of the ac specific heat to a model landscape incorporated with the distribution of the transition rate exploited in the trapping diffusion model^{7,19}.

We prepare a landscape consisting of 20 basins which are mutually connected. The microscopic dynamics of the system in each basin is assumed to be the Debye oscillator. The free energy, F_i , of basin i is given by

$$F_i = \epsilon_i + \exp \left\{ 9 \left(\frac{T}{\Theta_D} \right)^3 \int_0^{\Theta_D/T} \ln \left(\frac{1}{2} \sin^{-1} \frac{x}{2} \right) x^2 dx \right\}, \quad (34)$$

where the energy ϵ_i of the bottom of basin i is uniformly distributed with the variance ϵ and Θ_D is the Debye temperature. Note that the form of the distribution does not play any important roles in the following discussion.

The energy, E_i , of basin i is calculated from the temperature derivative of the free energy F_i . The transition rate w is assumed to obey the power law distribution $P(w)$ as in the trapping diffusion model^{7,19},

$$P(w) = \begin{cases} \frac{\rho+1}{w_0} \left(\frac{w}{w_0} \right)^\rho & (0 \leq w \leq w_0) \\ 0 & \text{otherwise} \end{cases}, \quad (35)$$

where ρ is related to the configurational entropy $s_c(T)$ as

$$\rho = \frac{TS_c(T) - T_g S_c(T_g)}{T_g S_c(T_g)}. \quad (36)$$

The transition rate from basin j to i W_{ij} is now a random variable given by

$$W_{ij} = w_0 x^{\frac{1}{\rho+1}} \exp[-\beta(F_A(T) - F_j(T))]. \quad (37)$$

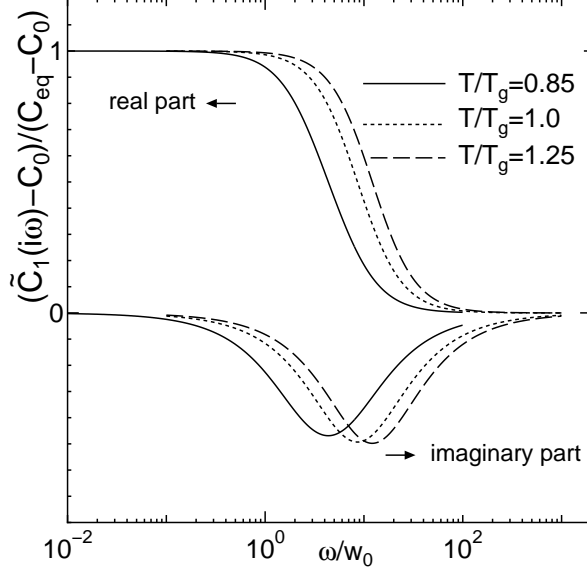


FIG. 2: The scaled ac specific heat in the trap model at the temperature $T/T_g = 0.85$ (solid line), 1.0 (dot line), 1.25 (dash line):

Here, x is the uniform random number in $[0, 1]$.

For numerical calculations in this study, the exponent ρ of the jump rate distribution is simplified as

$$\rho = \frac{T - T_g}{T_g - T_0}, \quad (38)$$

i.e. $S_c(T)$ is assumed as $TS_c(T) \propto T - T_0$ with the Vogel-Fulcher temperature $T_0 \sim T_k$ and the parameters are chosen as $T_0/T_g = 0.75$ and $\Theta_D/T_g = 12.5$, respectively. In addition, the crossover temperature T_x is $T_x/T_g = 1.25$ since the crossover temperature is identified with the exponent $\rho = 1.0$ ¹⁹.

B. The 1st-order ac specific heat

The real and imaginary parts of the scaled 1st-order ac specific heat $(\tilde{C}_1(i\omega) - C_0)/(C_{eq} - C_0)$ are shown in Fig.2. As the temperature is reduced, a peak of the imaginary part shifts to the low frequency region and the width of the peak increases.

Figure 3 shows the temperature dependence of the frequency ω_{peak} at the peak of the imaginary part. In the low temperature region below T_g , ω_{peak} obeys the power law function as $\omega_{peak} \sim (T - T_0)^{0.914}$. In the high temperature region above T_g , the temperature

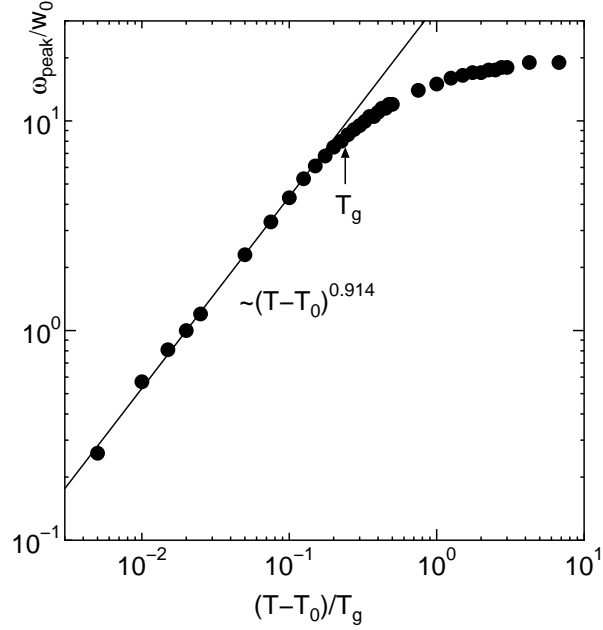


FIG. 3: The temperature dependence of the frequency at the peak of the imaginary part of the 1st-order ac specific heat: The peak frequency (black circle) becomes small as the temperature reduces toward the Vogel-Fulcher temperature T_0 . The line is fitted with the data in the low temperature region.

dependence changes and ω_{peak} approaches toward $20w_0$. It is straightforward to show that, when N basins are mutually connected, the ω_{peak} becomes Nw_0 in the high temperature region. In fact from Eq. (37), all transition rates are w_0 when the temperature is much higher than the glass transition temperature T_g . The relaxation time due to eigenvalues of transition matrix W is not distributed and the 1st-order ac specific heat becomes the same as the susceptibility of the Debye relaxation. The master equation (12) can be solved without difficulties in this limit as $P_i(T, t) = e^{-Nw_0 t} (P_i(t=0) - 1/N) + 1/N$. Thus the peak frequency ω_{peak} becomes Nw_0 in the high temperature region.

We define the stretching factor σ by the ratio $\sigma \equiv \omega_+/\omega_- (\omega_+ > \omega_-)$. Here, ω_{\pm} is the frequency satisfying the relation $\tilde{C}_1''(i\omega_{\pm}) = \tilde{C}_1''(i\omega_{peak})/2$. Figure 4 shows the temperature dependence of the stretching factor σ as a function of temperature. In the high temperature region above T_g , σ is the same as that of the Debye susceptibility. As the temperature is reduced toward T_0 , σ of the peak increases and diverges at T_0 . It means that the relaxation time is distributed and the broad peak appears in $\tilde{C}_1''(i\omega)$ below T_g . It is interesting to note

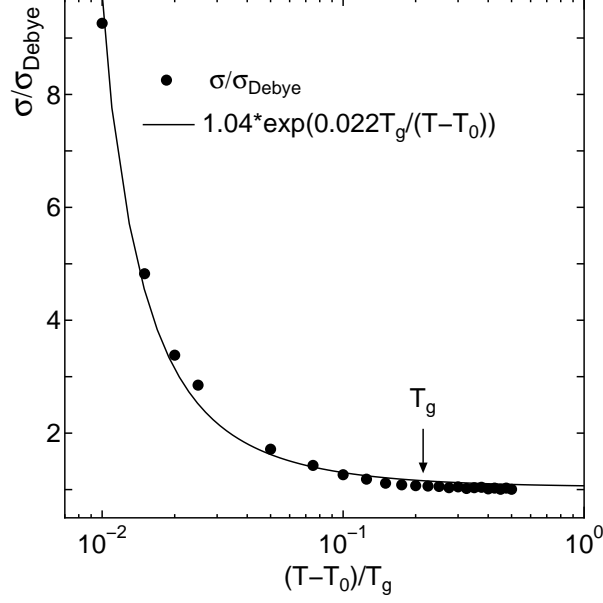


FIG. 4: The temperature dependence of the stretching factor σ of the imaginary part. The line represents the fitted line by Vogel-Fulcher law. Here, $\sigma_{Debye} = (2 + \sqrt{3})/(2 - \sqrt{3})$ is the stretching factor for the Debye relaxation type. As the temperature is reduced toward the Vogel-Fulcher temperature T_0 , σ increases.

that σ can be fitted well by the Vogel-Fulcher law as $\sigma \sim \exp(A/(T - T_0))$ shown in Fig.4.

The statistics of eigenvalues of the transition rate matrix W can be obtained from the frequency dependence of $\tilde{C}_1(i\omega)$. (See §IV B.) We show a result of comparison of $\lim_{\omega \rightarrow \infty} \omega \tilde{C}_1''(i\omega)/(C_{eq} - C_0)$, $\lim_{\omega \rightarrow \infty} \omega^2(\tilde{C}_1'(i\omega) - C_0)/(C_{eq} - C_0)$, and $\lim_{\omega \rightarrow 0} \omega^{-1} \tilde{C}_1''(i\omega)/(C_{eq} - C_0)$ with statistics of eigenvalues $\langle \lambda \rangle$, $\langle \lambda^2 \rangle$ and $\langle \lambda^{-1} \rangle$ in Fig.5. Here, $\langle f(\lambda) \rangle$ represents the statistics of eigenvalues as $\langle f(\lambda) \rangle = \sum_{i=1, \lambda_i \neq 0}^{20} f(\lambda_i)/20$, which is calculated numerically from the transition matrix W . The result indicates that the contribution of g_i is negligible and the coefficients obtained from the frequency dependence of the 1st-order ac specific heat can be used to estimate the statistics of eigenvalues of transition rate matrix.

Figure 6 shows the temperature dependence of $\lim_{\omega \rightarrow \infty} \omega \tilde{C}_1''(i\omega)/(C_{eq} - C_0)/W_0$, $\lim_{\omega \rightarrow \infty} \{\omega^2(\tilde{C}_1'(i\omega) - C_0)/(C_{eq} - C_0)/W_0^2\}^{1/2}$, and $\lim_{\omega \rightarrow 0} \omega(C_{eq} - C_0)/(\tilde{C}_1'(i\omega) - C_0)/W_0$ and the deviation between these statistics becomes significant below T_g . It reflects that the distribution of the eigenvalues becomes broader below T_g .

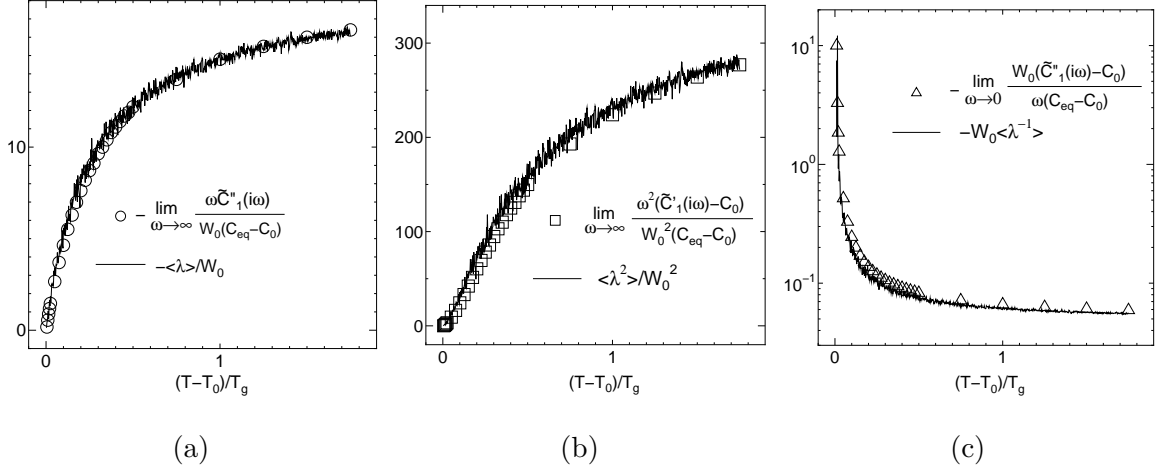


FIG. 5: The temperature dependence of (a) $-\lim_{\omega \rightarrow \infty} \omega \tilde{C}''_1(i\omega)/(C_{eq} - C_0)/W_0$, (b) $\lim_{\omega \rightarrow \infty} \omega^2(\tilde{C}'_1(i\omega) - C_0)/(C_{eq} - C_0)/W_0^2$, and (c) $-W_0 \lim_{\omega \rightarrow 0} \omega^{-1}(\tilde{C}''_1(i\omega) - C_0)/(C_{eq} - C_0)$ determined from the frequency dependence of the 1st-order ac specific heat. The solid lines represent (a) $-\langle\lambda\rangle/W_0$, (b) $\langle\lambda^2\rangle/W_0^2$ and (c) $-W_0\langle\lambda^{-1}\rangle$, which are calculated numerically from eigenvalues of the transition matrix W , respectively.

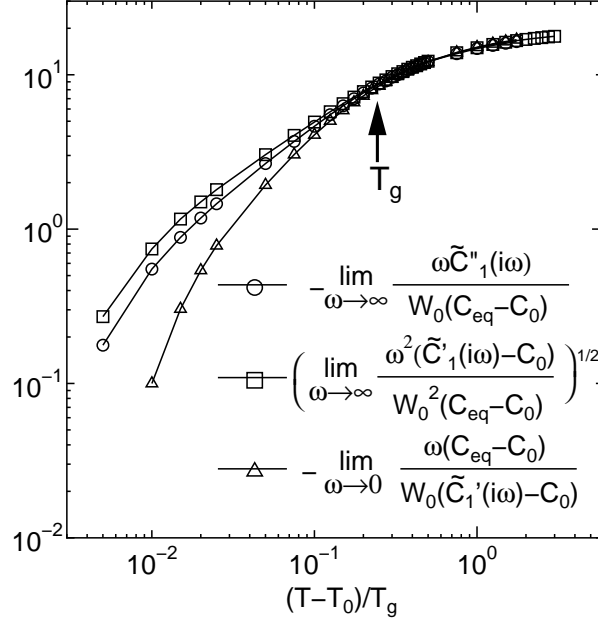


FIG. 6: The temperature dependence of $-\lim_{\omega \rightarrow \infty} \omega \tilde{C}''_1(i\omega)/(C_{eq}-C_0)/W_0$, $\lim_{\omega \rightarrow \infty} \{\omega^2(\tilde{C}'_1(i\omega) - C_0)/(C_{eq} - C_0)/W_0^2\}^{1/2}$, and $-\lim_{\omega \rightarrow 0} \omega(C_{eq} - C_0)/(\tilde{C}'_1(i\omega) - C_0)/W_0$. The deviation of these properties becomes significant below T_g .

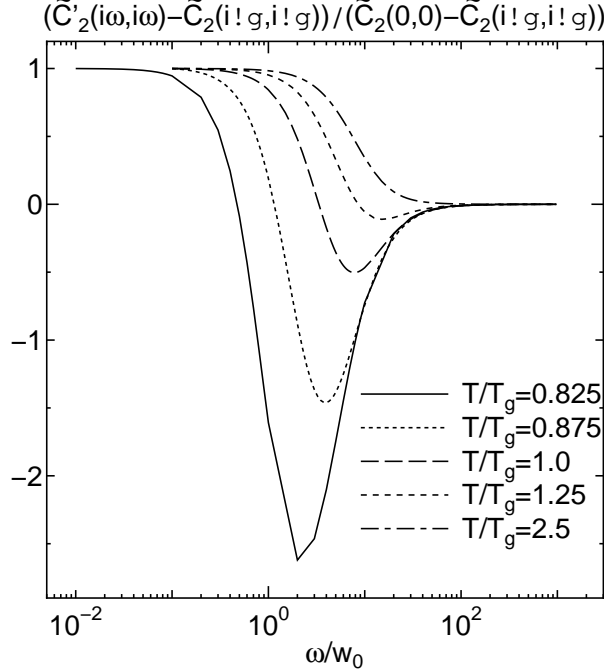


FIG. 7: The real part of the scaled 2nd-order ac specific heat at temperatures $T/T_g = 0.825, 0.875, 1.0, 1.25$ and 2.5 : As the temperature is decreased below the temperature $T_X/T_g = 1.25$, a local minimum decreases.

C. The 2nd-order ac specific heat

The real and imaginary parts of the scaled 2nd-order ac specific heat $(\tilde{C}_2(i\omega, i\omega) - \tilde{C}_2(i\infty, i\infty)) / (\tilde{C}_2(0, 0) - \tilde{C}_2(i\infty, i\infty))$ are shown in Fig. 7 and Fig. 8, respectively. The real part shows a decreasing local minimum when the temperature is reduced below the crossover temperature $T_X/T_g = 1.25$. It is important to note that the similar behavior is shown for the imaginary part in Fig.8, where the imaginary part has a decreasing minimum and an increasing maximum below the crossover temperature.

The deviation from the Debye relaxation appears clearly in the Cole-Cole plot of the 2nd-order ac specific heat shown in Fig.9. In the high temperature region, the plots show the semicircle, since the 2nd-order ac specific heat is equal to the susceptibility of the Debye relaxation. As the temperature is reduced, the plots deviate from the semicircle, that shows that the terms including $\partial W/\partial T$ in Eqs. (32) and (33) give significant contributions.

The temperature dependence of the extrema of the 2nd-order ac specific heat is shown

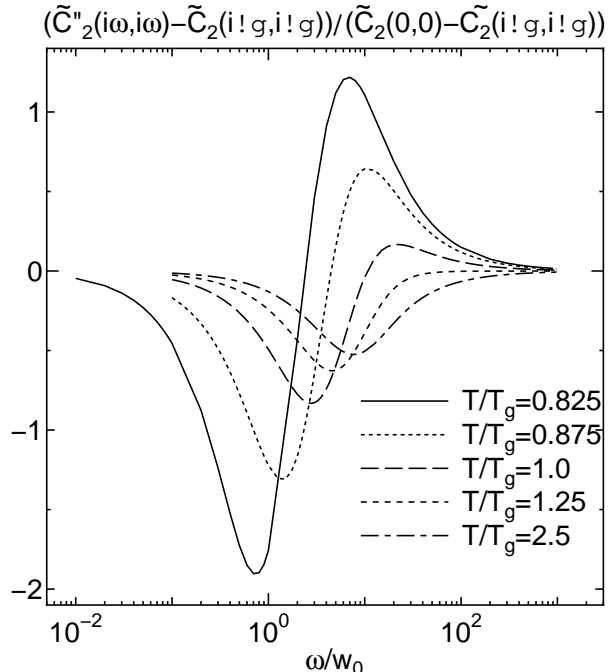


FIG. 8: The imaginary part of the scaled 2nd-order ac specific heat at temperatures $T/T_g = 0.825$, 0.875, 1.0, 1.25 and 2.5: As the temperature is decreased below the temperature $T_X/T_g = 1.25$, a local minimum decreases and a local maximum increases.

in Fig.10. Below T_g , the extrema obey the power law as $(T - T_0)^{-\nu}$, as the temperature is decreased toward T_0 . The exponents ν are $\nu = 0.97, 1.05, 1.01$ for the local maximum of the real part, the local minimum and the local maximum of the imaginary part, respectively. Above T_g , the temperature dependence of the minimum of the imaginary part deviates from the power law and approaches to a constant value.

VI. CONCLUSION

We presented the theoretical formalism of calculating the energy response to the oscillating temperature in the free energy landscape picture. The characteristic behaviors of the energy responses are summarized as follows.

The large and small frequency limits of the 1st-order ac specific heat are identical to the equilibrium and quenched specific heat in the free energy landscape picture, respectively. The distribution of the eigenvalues of the transition rate matrix among basins is shown to

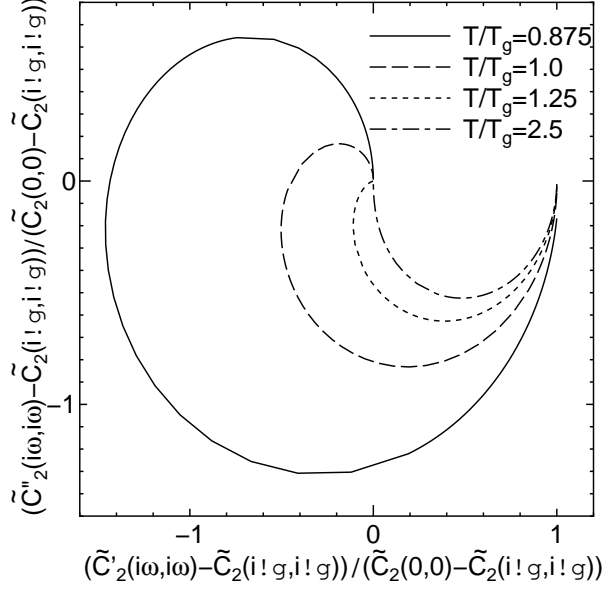


FIG. 9: The Cole-Cole plot of the scaled 2nd-order ac specific heat at temperatures $T/T_g = 0.875$, 1.0, 1.25 and 2.5: At a high temperature, the plots are semicircle. As the temperature is decreased, the plots deviate from the semicircle.

give rise to the broad peak of the imaginary part of the 1st-order ac specific heat. This is consistent with the experiment for the glass forming materials.

The 2nd-order ac specific heat is defined for the first time as the coefficient of the oscillating part of the 2nd-order energy response. The large and small frequency limits of the 2nd-order ac specific heat are identical to the temperature derivative of the annealed and quenched specific heat, respectively.

We analyzed the 1st- and 2nd-order ac specific heats for a model glass former on the basis of the free energy landscape picture and showed characteristics of the ac specific heats.

A frequency ω_{peak} at a peak of an imaginary part of the 1st-order ac specific heat shifts to the low frequency region as the temperature is decreased below the glass temperature T_g and approaches to 0 at the Vogel-Fulcher temperature T_0 . In the high temperature region above T_g , ω_{peak} becomes virtually independent of the temperature and approaches a constant value. A width of the peak becomes larger than that of the Debye relaxation type below T_g due to the distribution of the eigenvalue λ and diverges at T_0 . The statistics of λ such as $\langle \lambda \rangle$, $\langle \lambda^2 \rangle$, and $\langle \lambda^{-1} \rangle$ can be obtained from the frequency dependence of the 1st-order ac specific heat, and these quantities shows deviation from the Debye-type

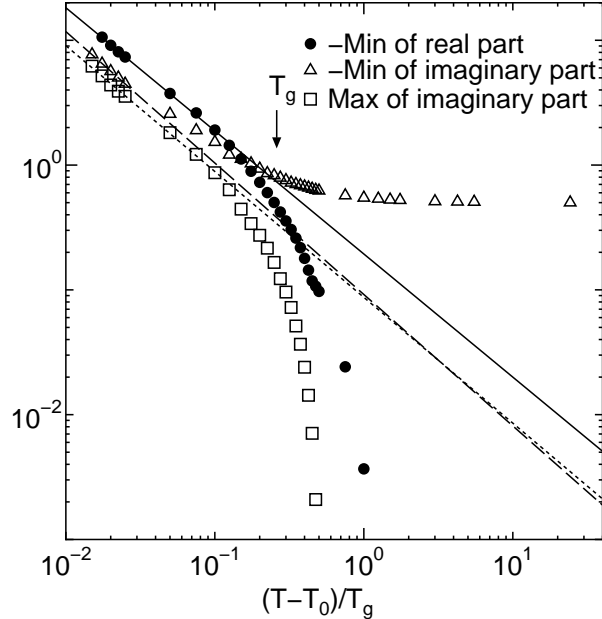


FIG. 10: The temperature dependence of the extrema of the scaled 2nd-order ac specific heat: The lines are fitted by power law functions in the low temperature region. Below T_g , the extrema obeys the power law as $(T - T_0)^{-\nu}$. Above T_g , the temperature dependence of the extrema shows significant changes.

relaxation below T_g .

The scaled 2nd-order ac specific heats have extrema, which obey the power law as $(T - T_0)^\nu$ below T_g . Above T_g , the temperature dependence of the extrema changes. The local minimum of the real part and the local maximum of the imaginary part vanish and the local minimum of the imaginary part approaches to the constant value near the crossover temperature T_x .

In conclusion, the characteristics of the transition rate among basins reflect the frequency dependence of the 1st- and 2nd-order ac specific heats. It means that the glass transition point T_g , the Vogel-Fulcher temperature T_0 and the crossover temperature T_x can be determined from the 1st- and 2nd-order ac specific heats. It is interesting to note that we can determine T_0 , at which the shear viscosity diverges, i.e. a dynamically defined characteristic temperature, from the thermodynamic measurement as the 1st- and 2nd-order energy response.

Acknowledgments

We would like to thank Professors Y. Saruyama, O. Yamamuro and A. Yoshimori for useful discussions on this study. This work was supported in part by a Grand-in-Aid for Scientific Research from the Ministry of Education, Culture, Sports, Science and Technology.

- * Electronic address: f.tagawa@cmt.phys.kyushu-u.ac.jp
- ¹ G. E. Gibson and W. F. Giaque, *J. Am. Chem. Soc.* **40**, 93 (1923).
- ² M. Mézard and G. Parisi, *J. Chem. Phys.* **116**, 1076 (1999).
- ³ M. Goldstein, *J. Chem. Phys.* **51**, 3728 (1969).
- ⁴ F. Sciortino, *J. Stat. Mech.* Art. No. P5015 (2005).
- ⁵ T. Odagaki, T. Yoshidome, A. Koyama and A. Yoshimori, *J. Non-Crys. Solids.* **353**, 4843 (2006)
- ⁶ T. Odagaki and T. Ekimoto, submitted to *J. Non-Crys. Solids* (2007).
- ⁷ T. Odagaki and Y. Hiwatari, *Phys. Rev. A.* **41**, 929 (1991).
- ⁸ T. Odagaki, T. Yoshidome, T. Tao, and A. Yoshimori, *J. Chem. Phys.* **117**, 10151 (2002).
- ⁹ T. Odagaki, T. Tao and A. Yoshimori, *J. Non-Cryst. Solids.* **307-310**, 407 (2002).
- ¹⁰ T. Tao, A. Yoshimori and T. Odagaki, *Phys. Rev. E.* **66**, 041103 (2002).
- ¹¹ T. Tao, T. Odagaki and A. Yoshimori, *J. Chem. Phys.* **122**, 044505 (2005).
- ¹² D. Chakrabarti and B. Bagchi, *J. Chem. Phys.* **120**, 11674 (2004).
- ¹³ D. Chakrabarti and B. Bagchi, *J. Chem. Phys.* **122**, 014501 (2005).
- ¹⁴ F. Tagawa and T. Odagaki, *J. Phys. Soc. Jpn.* **75**, 124003 (2006).
- ¹⁵ O. Yamamuro, I. Tsukushi, A. Lindqvist, S. Takahara, M. Ishikawa and T. Matsuo, *J. Phys. Chem.* **B102**, 1605 (1998).
- ¹⁶ N. O. Birge and S. R. Nagel, *Phys. Rev. Lett.* **54**, 2674 (1985).
- ¹⁷ T. Christensen, *J. Phys.(Paris) Colloq.* **46**, C8-635(1985).
- ¹⁸ J K. Nielsen and J C. Dyre, *Phys. Rev. B.* **54**, 15754(1996).
- ¹⁹ T. Odagaki, *Phys. Rev. Lett.* **75**, 003701(1995); T. Odagaki, *Prog. Theor. Phys. Suppl.* **126**, 9(1997).